Triplet Dynamics of Conformationally Distorted Porphyrins in Isotropic Liquids and Liquid Crystals. Time-Resolved Electron Paramagnetic Resonance Study

Shalom Michaeli, Shay Soffer, and Haim Levanon*

Department of Physical Chemistry and The Farkas Center for Light-Induced Processes, The Hebrew University of Jerusalem, Jerusalem 91904, Israel

Mathias O. Senge and Werner W. Kalisch

Institut für Organische Chemie (WE02), Freie Universität Berlin, Takustrasse 3, D-14195, Berlin, Germany

Received: September 17, 1998; In Final Form: January 8, 1999

The photoexcited triplet states of four nonplanar (distorted) porphyrins were examined by laser excitation−time-resolved EPR spectroscopy. The compounds examined were 2,3,7,8,12,13,17,18-octaethyl-5,10,15,20-tetraphenylporphyrin (H_2OETPP); 2,3-diethyl-5,10,15,20-tetraphenylporphyrin (H_2DETPP); 2,3,12,13-tetraethyl-5,10,15,20-tetraphenylporphyrin (H_2*t*TETPP); and 2,3,7,8-tetraethyl-5,10,15,20-tetraphenylporphyrin (H_2*c*TETPP). Measurements were carried out at low temperatures in glassy isotropic matrixes and over a wide temperature range in a uniaxial LC (liquid crystal, E-7). The triplet states of H_2*t*TETPP, H_2*c*TETPP, and H_2OETPP are characterized by relatively small zero-field splitting (ZFS) values, *D*, compared to free base porphyrin (H_2-TPP). For the H_2OETPP the relation $D \sim 3E$ between the ZFS parameters was observed. In the case of H_2DETPP the ZFS parameter *D* was found to be larger relative to H_2TPP. Line shape analyses indicate that the triplet spectra depend on the specific chromophore, the temperature, and the LC phase. The results in LC suggest that intermolecular triplet energy transfer occurs in all four chromophores, and in the case of H_2-OETPP there is evidence for the simultaneous presence of two types of triplets (different saddle conformers of H_2OETPP), which are identical in their ZFS parameters. To check on the sign of *D* and triplet spin alignment, the photoexcited triplet states in isotropic solvents were investigated by fast EPR−magnetophotoselection through the determination of the position of the optical transition moment. These experiments allow determining the location of the optical transition moment and the triplet spin alignment.

I. Introduction

Crystallographic data of reaction centers (RCs) suggest that the *bacteriochlorophylls* (*Bchl*) assume different conformations, which exhibit significant departures from strict planarity.[1,2] Deviations from planarity were also found in porphyrins (Ni(II), Cu(II), Co(II), Zn(II)),[3,4,16] chlorins, and bacteriochlorins as isolated molecules and in protein environment.[5,6] The considerable flexibility of isolated porphyrinoids allows for significant distortions, that can be imposed on these macrocycles by crystal packing and steric effects.[6,7] These studies have led to the concept of "conformationally designed" porphyrins in which multiple peripheral substituents induce large deformations of the macrocycle that minimize steric interaction between the substituents.[8−11] Theoretical calculations indicate that the conformational variations shift the frontier orbitals of the chromophores and thereby can modulate the redox and optical properties.[8,9] A conspicuous example is the free-base derivatives of 2,3,7,8,12,13,17,18-octaethyl-5,10,15,20-tetraphenylporphyrin (H_2OETPP),[10] which can assume severe saddled conformations, in which the pyrrole rings move alternately up and down and the phenyl rings rotate into planes of the macrocycles with an average angles of ∼45° with respect to the porphyrin plane. In addition, NMR measurements in solution suggest the flipping of opposite pyrrole rings to the other side of the porphyrin plane.[4,10,12]

Unlike X-ray and NMR studies of the conformational distorted porphyrins in their ground state, data on their properties in the photoexcited triplet state are scarce. Such data are of prime importance since the conformational deviations from planarity should be related to changes of the excited states properties of the distorted porphyrins compared to that of the planar H_2TPP. For example, relative to H_2TPP the triplet yield of H_2OETPP is significantly smaller,[13] the fluorescence Stokes shift of H_2-OETPP is large (∼500 cm^{-1}) and the lifetime of the lowest excited singlet state is reduced.[14] A direct approach of studying the excited states of the porphyrins is via their magnetic parameters in the excited triplet states. A first study employing time-resolved EPR (TREPR) spectroscopy to determine possible conformational changes of distorted porphyrins, embedded in liquid crystals (LCs), was reported earlier.[15] Changes of the triplet line shape were directly related to the conformational changes in H_2OETPP and ZnOETPP.

The present study is an extension of our previous work, investigating the photoexcited triplet states of 2,3-diethyl-5,10,15,20-tetraphenylporphyrin (H_2DETPP), 2,3,7,8-tetraethyl-5,10,15,20-tetraphenylporphyrin (H_2*c*TETPP), 2,3,12,13-tetraethyl-5,10,15,20-tetraphenylporphyrin (H_2*t*TETPP) and 2,3,7,8,12,13,17,18-octaethyl-5,10,15,20-tetraphenylporphyrin (H_2-OETPP) in an isotropic glassy matrix (toluene) and in an anisotropic nematic LC (Figure 1). In addition to the unique dielectric properties of LC, it serves here as a simplified model description of the in vivo effects by the organized protein environments. Furthermore, the triplet state dynamics can be studied by EPR over a wide temperature range,[16−18] not possible

10.1021/jp983772e CCC: $18.00
Published on Web 04/01/1999

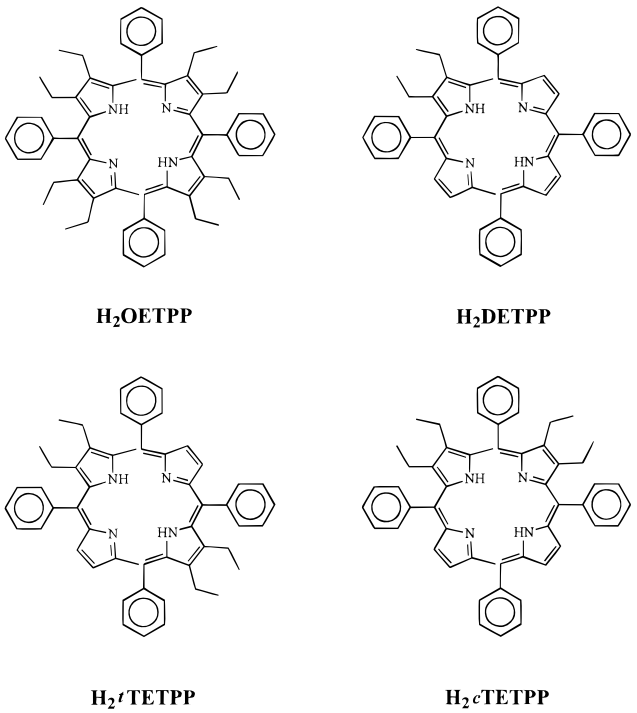

Figure 1. Structures of the distorted porphyrins.

in isotropic toluene solution because of the large broadening of the EPR lines (fast relaxations) in the liquid phase of toluene. Line shape analysis of the triplet EPR spectra in the LC as a function of temperature suggests exchange (hopping) processes between the magnetic frames of reference of two identical interacting chromophores. We have also demonstrated, by EPR−magnetophotoselection (MPS), that molecular distortions lead to significant changes of triplet spin alignment and changes in the location of the optical transition moment (**M**) compared to traditional porphyrins. It should be pointed out that since all of the investigated porphyrinoids are nonplanar, the term molecular plane is meaningless, and therefore we shall be using the zero-field-splitting (ZFS) frame of reference. Analysis of the results enables to determine the following: (i) the relation between the molecular and dipolar frame of references, from which the sign of the ZFS parameter, *D*, was found to be positive and (ii) the relation between the molecular frame of reference and **M**, which was found to be located out of the *XY* plane of the ZFS tensor in all four investigated chromophores. We, thus, find that selective light excitation combined with TREPR spectroscopy provides a most sensitive method for elucidating spectroscopic properties associated with the triplet states of distorted porphyrins.

II. Experimental Section

H_2DETPP, H_2*t*TETPP, H_2*c*TETPP, and H_2OETPP (Figure 1) were synthesized as reported previously.[10,19] Toluene (Baker Analyzed) was dried over molecular sieves. Liquid crystal (E-7) from BDH was used without further purification.[20] E-7 is characterized by the following phase transition temperatures:

$$\text{crystalline} \xleftrightarrow{210\ \text{K}} \text{soft crystalline} \xleftrightarrow{263\ \text{K}} \text{nematic} \xleftrightarrow{333\ \text{K}} \text{isotropic} \quad (1)$$

EPR samples of the porphyrins ($\sim 10^{-3}$ M) dissolved in toluene and LC were prepared in Pyrex tubes, degassed by freeze−vacuum−thaw cycles, and sealed under vacuum. The LC samples were prepared in similar tubes by first introducing the chromophores in toluene solution, evaporating off the solvent, and then introducing the LC followed by degassing and finally sealing the sample. Continues wave-EPR, diode detection measurements were carried out on a Bruker ESP 380 (*X*-band) interfaced to a dye laser (Continuum, TDL-60) pumped by Nd:Yag laser (Continuum, 661-2D) producing a 20 Hz pulse of $\sim$12 mJ/pulse. To verify the results, identical experiments were performed on a Varian (E-12) EPR spectrometer. The excitation wavelengths of 560 and 532 nm were chosen according to the Q-band optical transitions of chromophores. No wavelength dependence of the results were noticed. The temperature was maintained by a nitrogen flow system. Detailed description of light excitation, signal detection, and the real-time data acquisition are given elsewhere.[21,22]

EPR experiments using LC were performed at two configurations where the director, **L**, is parallel (**L**∥**B**) or perpendicular (**L**⊥**B**) to the external magnetic field, B. MPS experiments were carried out by utilizing two light-polarized excitations, i.e., where the dominant electric field components are either vertically (**E**⊥**B**) or horizontally polarized (**E**∥**B**). Changing from the initial vertical polarization into the horizontal one was carried out by utilizing a set of one mirror and four prisms, located at different planes. A commercial polarizer, keeping the same intensity for two polarizations verified the final polarization in front of the EPR cavity. Detailed description of the MPS experiments are given elsewhere.[23−25]

III. Theory

EPR line shape analysis of photoexcited triplets oriented in isotropic or anisotropic matrixes, including dynamic processes is described elsewhere.[16,17,21,26] Therefore, in the present paper we briefly outline the main features of the analysis. For randomly oriented chromophores, the EPR line shape can be expressed by the imaginary part of the magnetic susceptibility,[21,27]

$$\chi''(\mathbf{B},t) \propto \sum_{\substack{i=1,2 \\ j=i+1}} \int_0^{\pi/2} \int_0^{\pi/2} \text{Im}[(\rho_{ij}(\theta,\varphi,\text{t})]\, D(\theta,\varphi) \quad (2)$$

where θ and φ are the angles between the external magnetic field, **B**, and the principal axis system of the magnetic dipolar tensor, $\rho_{ij}(\theta,\varphi,t)$ is the density matrix element connecting the *i*, *j* levels. $D(\theta,\varphi) = \sin\theta\ \mathrm{d}\theta\ \mathrm{d}\varphi$ is the distribution function for unpolarized light excitation. The summation is over the two possible transitions and, because of symmetry, the integration is carried out over one octant of space.

For unpolarized light and cylindrical distribution of the guest compound about the director, **L**, the EPR line shape is given by[21,27]

$$\chi''(\mathbf{B},t) \propto \sum_{\substack{i=1,2 \\ j=i+1}} \int_0^{\pi/2} f(\grave{\theta}) \int_{\theta\,\text{min}}^{\pi/2} \int_0^{\pi/2} \text{Im}[(\rho_{ij}(\theta,\varphi,\text{t})] \times \mathrm{f}(\varphi)\ \mathrm{d}\theta\ \mathrm{d}\varphi\ \mathrm{d}\grave{\theta} \quad (3)$$

where in this case $D(\theta,\varphi) = 1$, and $\theta_{\text{min}} = (\pi/2) - \chi \pm \grave{\theta}$. The sign of $\grave{\theta}$ is chosen such that $0 \le \theta_{\text{min}} \le \pi/2$, and χ is the angle of the sample rotation about an axis perpendicular to **B**. The distribution functions $f(\phi)$ and $f(\grave{\theta})$ express the fluctuations of the molecules about **L**. The Gaussian $f(\phi)$ is characterized by a variance σ_ϕ^2, for rotating the molecule by an angle ϕ, about the axis perpendicular to the *X*, *Y* plane, with a preferred

orientation at the angle ϕ_0. The fluctuations of the *X, Y* plane about **L** are expressed by $f(\dot{\theta}) = \cos^2(\dot{\theta}) \exp(-\dot{\theta}^2/\sigma_\theta^2)$.

Utilization of eq 3 without taking into account dynamic effects could not provide satisfactory results. An example of triplet dynamics is intermolecular exchange of the principal axes of the dipolar tensor in terms of solidlike discrete jumps. Such a mechanism accounts for triplet hopping between two sites characterized by separate frames of reference X_A, Y_A, Z_A, and X_B, Y_B, Z_B. The relation between the two principal-axes systems of A and B sites is expressed by the Euler rotation matrix.[17] The contribution of the exchange process to the line shape expression of eq 2 is given by:

$$\rho_{ij} = \rho_{ij}^{AB} \sim (\rho_{jj} - \rho_{ii})(\rho_{jj}^{A} + \rho_{ii}^{B}) \quad (4)$$

where $(\rho_{jj} - \rho_{ii})$ is the population difference of the polarized triplet sublevels. The terms ρ_{jj}^{A} and ρ_{jj}^{B} describe the probability for an EPR transition and depend on the Zeeman and dipolar interactions of each site, as well as on the exchange rate, **k.** In addition to the triplet magnetic parameters, the analysis results in the relative orientation of the two configurations and the triplet hopping rate.[18,28]

Upon application of the MPS method, the distribution function should be modified. In such a case, the ensemble of triplet states excited by polarized light is derived from the probability that the optical transition moment **M** is related to the electric field component, **E**, through the relation **E**||**B** or **E**⊥**B**. Knowing the location of **M** is highly important for determination of singlet−singlet transition character, e.g., $\pi\pi^*$ or $n\pi^*$. Thus, the distribution functions are given by

$$D_{\mathbf{E}\|\mathbf{B}} = (P_x \sin\theta\cos\varphi + P_y \sin\theta \sin\phi + P_z \cos\theta)^2 \sin\theta \, d\theta \, d\varphi \quad (5)$$

$$D_{\mathbf{E}\perp\mathbf{B}} = {}^1/_2[1 - (P_x \sin\theta\cos\varphi + P_y \sin\theta \sin\phi + P_z \cos\theta)^2] \sin\theta \, d\theta \, d\varphi \quad (6)$$

where P_i $(i = x, y, z)$ represents the projections of **M** onto the three principal magnetic axes, given by

$$P_x = \sin\gamma\cos\delta; \qquad P_y = \sin\gamma\sin\delta; \qquad P_z = \cos\gamma \quad (7)$$

where γ is the angle between the **M** and the out-of-plane (*X, Y*) magnetic axis and δ is the angle between the in-plane principal axis and the projection of **M** onto the *X, Y* plane. The relation between the laboratory and magnetic frame of references and **M** are presented in Figure 2.

The relaxation times of the triplet EPR signals were extracted from the analysis of the magnetization time profiles, $M_y(t)$, using the exponential expression:[29,30]

$$M_y(t) = \omega_1(e^{-c_+ t} - e^{-c_- t})/(c_- - c_+) \quad (8)$$

with the definitions:

$$c_+ = {}^1/_2(T_1^{-1} + T_2^{-1}) - [(T_2^{-1} - T_1^{-1})^2/4 - \omega_1^2]^{1/2}$$

$$c_- = {}^1/_2(T_1^{-1} + T_2^{-1}) + [(T_2^{-1} - T_1^{-1})^2/4 - \omega_1^2]^{1/2} \quad (9)$$

where ω_1 is the microwave power and $T_{1,2}$ are spin−lattice and spin−spin relaxation times.

IV. Results and Discussion

i. Triplet State in E-7. *(a) General Information.* In Figures 3 and 4 we show the triplet EPR spectra of H_2DETPP, H_2tTETPP, H_2cTETPP, and H_2OETPP oriented in E-7 at 140 K at **L**||**B** and **L**⊥**B** orientations. Similar to planar porphyrins in nematic LCs,[21,25,31,32] the spectra of the distorted porphyrins reveal an anisotropic triplet distribution, which depends on the orientation of **L** with respect to **B**. Compared to H_2TPP (the control compound) that exhibits a polarization pattern of **e,e,e,a,a,a** from low to high field, the polarization patterns are **e,a,e,a,e,a** for H_2DETPP and **a,a,a,e,e,e** for H_2cTETPP, H_2tTETPP, and H_2OETPP[33] (**e** stands for emission and **a** for absorption). The different polarization patterns of the triplet spectra indicate the different selective population rates, $T_i \leftarrow S_1$ $(i = x, y, z)$ of the triplet sublevels. The magnetic parameters extracted from the line shape analysis (Table 1) indicate that $D_{(H_2DETPP)} > D_{(H_2TPP)}$, while $E_{(H_2DETPP)} < E_{(H_2TPP)}$. On the other hand, the ZFS parameters of H_2tTETPP, H_2cTETPP, and H_2-OETPP obey the relation $D_{(H_2TPP)} > D_{(H_2tTETPP)} > D_{(H_2cTETPP)} > D_{(H_2OETPP)}$, and $E_{(H_2tTETPP)} > E_{(H_2OETPP)} \approx E_{(H_2TPP)} > E_{(H_2cTETPP)}$. It is evident, that the ZFS parameters are strongly affected by the substituents, which may change the spin density distribution. In the case of the H_2DETPP the strong dipolar interaction indicates a decrease of the effective distance between the triplet

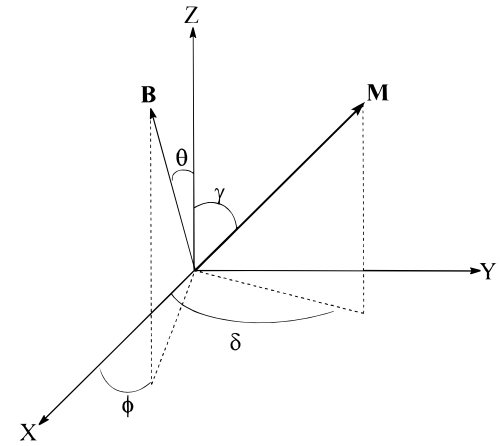

Figure 2. Relationship between the external magnetic field, **B**, optical transition moment **M** and ZFS magnetic axes system *X, Y, Z*. The external magnetic field, **B**, is defined by θ and ϕ and the optical transition moment, **M**, is defined by γ and δ.

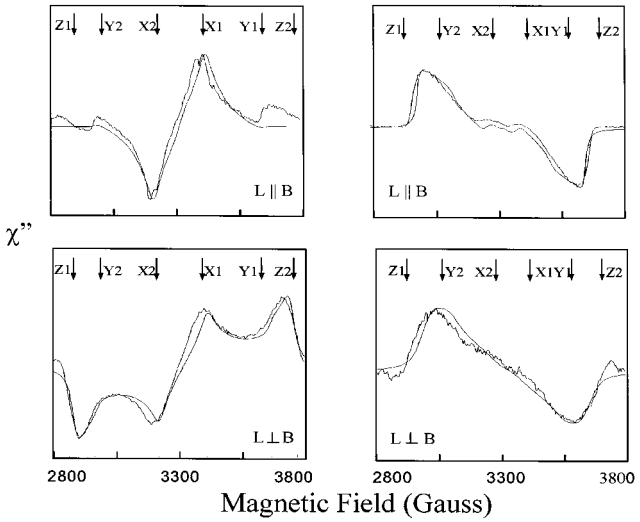

Figure 3. Direct detection TREPR spectra (taken at 850 ns after the laser excitation pulse) of H_2DETPP (left) and H_2tTETPP (right) oriented in E-7 at **L**||**B** and **L**⊥**B**. Spectra were taken at $T = 140$ K and at 50 mW microwave power. Laser excitation at 532 nm, 12 mJ/pulse. The superimposed smooth lines are computer simulations according to eq 2 (Table 1).

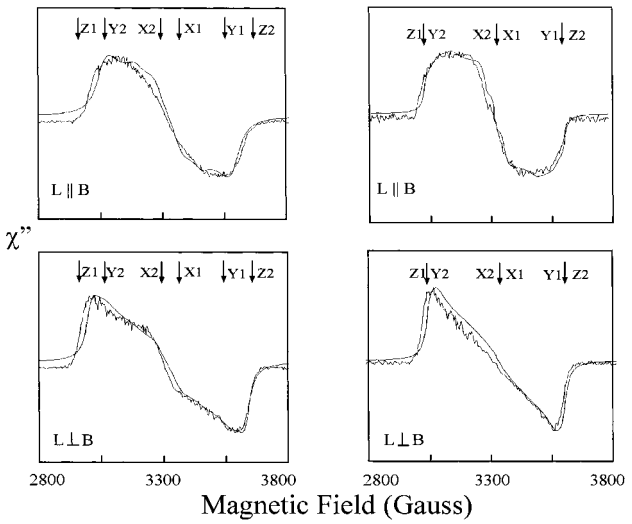

Figure 4. Direct detection TREPR spectra (taken at 850 ns after the laser excitation pulse) of H_2*c*TETPP (left) and H_2OETPP (right) oriented in E-7 at **L**‖**B** and **L**⊥**B**. Experimental conditions and analysis are as in Figure 3.

TABLE 1: Magnetic Parameters of Distorted Porphyrins at 140 K in E-7

compound	D[a]	$\|E\|$[a]	A_x:A^y:A_z
H_2TPP[b]	371	90	1:0.6:0.3
H_2DETPP	422	81	1:0.6:0.3
H_2cTETPP	305	70	0.3:0.4:1
H_2tTETPP	330	100	1:0:1
H_2OETPP[b]	277	92	0.2:0.5:1

[a] $\times 10^{-4}$ (cm^{-1}) (error ±5). [b] Taken from ref.[15]

electrons. On the other hand, the decreased value of ZFS parameter *D* in H_2*t*TETPP, H_2*c*TETPP, and H_2OETPP indicates increased delocalization of the triplet electrons. In the case of H_2OETPP, the result $|D| \sim 3|E|$ (Table 1) corresponds to a triplet spectrum, where two principal axes (*Z* and *Y*, or *Z* and *X*), depending on the signs of *D* and *E*, fall at the same field position. It is noteworthy to add that except for H_2DETPP, the other three chromophores undergo intermolecular exchange processes, also at the lowest temperature of our experiments, $T = 140$ K. In the following sections we discuss separately the results of each porphyrinoid.

(b) H2DETPP in LC. The triplet line shape associated with H_2DETPP at **L**‖**B** depends on the temperature, i.e, the LC phase, and most interestingly on the time interval between the laser pulse and EPR detection (Figure 5). In Figure 5a, we show the triplet EPR spectrum of the H_2DETPP detected at 140 K, 485 ns after the laser pulse. The polarization pattern of this spectrum is **e,a,e,a,e,a**, and remains the same over the entire decay time of the magnetization, $M_y(t)$, up to 190 K. Upon raising the temperature, two conspicuous effects are noticed. First, in the range $190 \leq T \leq 255$ K, while the polarization pattern is unchanged (**e,a,e,a,e,a**), the line shape of the detected spectrum changes particularly at the *Y* canonical orientation. Second, as seen from Figure 5b,c at $T \geq 255$ K the polarization pattern **e,a,e,a,e,a**, which is observed at early times, evolves into a polarization pattern of **e,e,e,a,a,a.** This is also reflected by the kinetic profiles, taken at different canonical orientations (Figure 5). It is inconceivable that $T_i \leftarrow S_1$ population rates are modified and are responsible for these spectral changes. In other words, an additional mechanism, which affects the line shape should be considered.

Line shape analysis of the triplet spectrum at low temperatures, e.g., $T \cong 140$ K leads to the relative population rates of

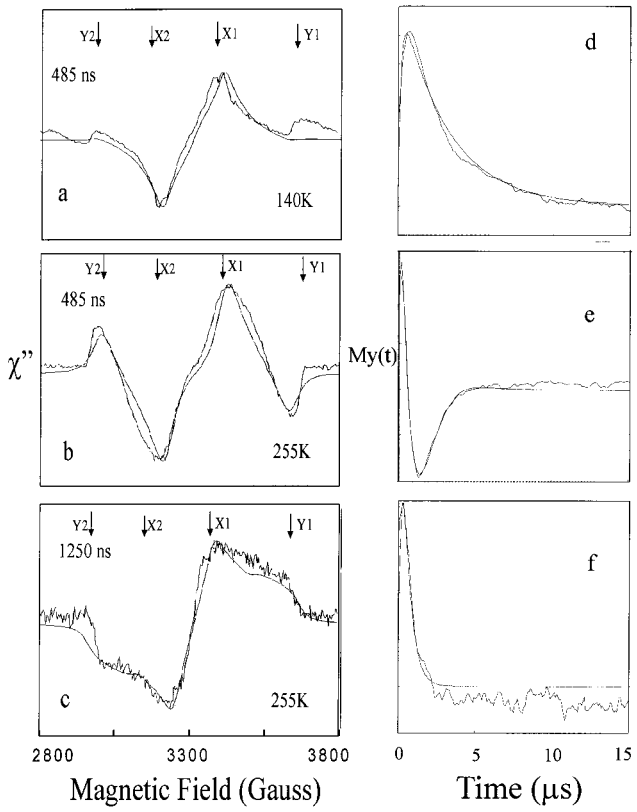

Figure 5. Temperature dependence of TREPR spectra of H_2DETPP oriented at **L**‖**B** in E-7. All experimental conditions are as in Figure 3. The superimposed smooth curves are computer simulations according to eq 2 with parameters presented in Tables 1 and 2. The corresponding temporal behavior of the magnetization $M_y(t)$, taken at *X*1 canonical orientation (d). Kinetic traces at *Y*2 (e) and X1 (f) canonical orientations were taken at 255 K. The solid lines (d) and (f) were determined by using eqs 8 and 9 with $1/T_1 = 0.17 \times 10^6$ s^{-1}, $1/T_2 = 0.44 \times 10^6$ s^{-1} and $1/T_1 = 1.23 \times 10^6$ s^{-1}, $1/T_2 = 4.1 \times 10^6$ s^{-1} at 140 and 255 K, respectively; trace (e) was simulated by eq 10. The minimum point in the decay curve (e) corresponds to ~1460 ns, and the constant signal intensity in the decay curves (d) and (f) represents the signal in thermal distribution.

A_x:A_y:A_z = 1:0.6:0.3. On the other hand, at 190 K ≤ T ≤ 255 K, the population rates extracted from the line shape analysis are A_x:A_y:A_z = 1:0.15:0.3. This change in population rates is insufficient to modify drastically the polarization pattern and the triplet line shape. The small difference in population rates at the two temperatures may be attributed to increased molecular fluctuations of the chromophore upon increasing the temperature.

As indicated above, close to the soft glass-nematic phase transition temperature ($T \geq 255$ K) a clear polarization change is noticed. The spectrum observed at the time window of 1250 ns after the laser pulse was simulated with the relative population rates of the triplet sublevels, A_x:A_y:A_z = 1:0.83:0.25 as compared to A_x:A_y:A_z = 1:0.15:0.3 at 485 ns. To account for this unusual observation, two mechanisms should be considered: transfer of polarization between interacting chromophores through different principal axes[34] and polarization inversion.[35]

Applying the first mechanism to our case, the polarization transfer between the neighboring chromophores may occur due to mixing between *X* and *Y* principal axes. As a result, population from the overpopulated *X* axis is transferred to the *Y* axis, thus changing the population ratio of the triplet sublevels, which leads to the different line shapes of the detected triplets. The second mechanism was applied to the triplet dynamics and polarization inversion of fullerenes and other organic com-

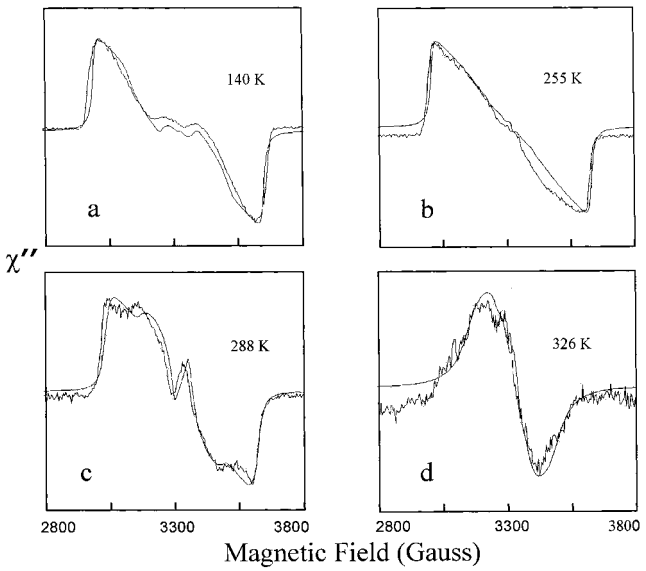

Figure 6. Temperature dependence of TREPR triplet spectra (**L**||**B**) of H_2*t*ETPP in the crystalline and nematic phases of E-7, taken at 850 ns after the laser pulse. Other experimental conditions are as in Figure 3. The superimposed smooth curves are computer simulations according to eqs 2 and 3 with parameters presented in Tables 1 and 2.

pounds.[35] This mechanism is associated with anisotropic decay rates to the ground state. For the case $D > 0$, i.e., $X > Y > Z$, and sufficiently large for k_z, the two corresponding transitions of the *Y* canonical orientation should exhibit polarization inversion. It should be emphasized that these arguments are valid only when the rate of phase inversion is greater than the spin−lattice relaxation rate. Unfortunately, at this stage we cannot rule out either of the proposed mechanisms. In particular, in view of the fact that such a behavior is unique to H_2DETPP.

The magnetization time profiles, $M_y(t)$, detected at the canonical orientations *X*1 and *Y*2 of the triplet spectrum are presented in Figure 5. The magnetization curve detected at field position *Y*2 exhibits a biphase behavior. If spectrum c evolves from spectrum b, then the rise time of spectrum c should be equal to the decay time of spectrum b. Thus, the observed signal as a function of time is expressed by

$$I(t) = -A\exp(-t/\tau_1) + B\exp(-t/\tau_2) - C(1 - \exp(-t/\tau_2))\exp(-t/\tau_3) \quad (10)$$

where *A*, *B* and *C* are the EPR signal amplitudes of the consecutive processes: a rise with the characteristic time τ_1 followed by the decay τ_2 of the early signal and the rise time of spectrum c with τ_2, and the final magnetization decay time is characterized by τ_3. The characteristic rates, extracted by the best fit analysis of the kinetic curve, presented in Figure 5 are $k_1 = 1/\tau_1 = 2.3 \times 10^6\ s^{-1}$, $k_2 = 1/\tau_2 = 2.54 \times 10^6\ s^{-1}$, and $k_3 = 1/\tau_3 = 0.78 \times 10^6\ s^{-1}$. The spin−lattice relaxation rate $1/T_1$, determined from the kinetic curve (e, f) taken at the canonical orientation *X*1 is $1/T_1 = 1.23 \times 10^6\ s^{-1}$ (eqs 8 and 9), satisfying the condition $k_2 > 1/T_1$.

(c) H_2tTETPP and H_2cTETPP in LC. The triplet spectra of H_2*t*TETPP also exhibit a gradual changes with temperature, but without phase inversion, as discussed above. As will be shown below, these changes are attributed to an intermolecular exchange process between neighboring molecules in the LC matrix in terms of their dipolar axes. Triplet EPR spectra of H_2*t*TETPP at different temperatures at the **L**||**B** are presented in Figure 6.[36] It is noticeable that the triplet spectra start to change in the soft crystalline phase of the LC. Moreover, the

TABLE 2: Dynamic Parameters for Triplet States of Distorted Porphyrins in E-7 (L||B)

	H_2TETPP		H_2*t*TETPP		H_2OETPP	
T^a	k^b	α_X:α_Y:$\alpha_Z{}^c$	k^b	α_X:α_Y:$\alpha_Z{}^c$	k^b	α_X:α_Y:$\alpha_Z{}^c$
140	1.4	0:40:90	1.4	0:35:0	0.56	10:10:90
255			1.4	0:50:0	0.56	10:30:90
268	2.8	0:10:90			0.56	10:30:90
288	5.6	0:0:90	1.4	0:25:45		
298	7	0:0:90				
326			33.6	0:55:50	19.6	0:80:0

[a] ±2 K. [b] $\times 10^7\ s^{-1}$. [c] Euler angles in degrees (error ± 5°).

magnetic, spin dynamics, and distribution parameters extracted from the low-temperature spectra are insufficient to account for the conspicuous temperature dependence of the spectra. As reported in previous studies,[15,18,28] the reduction of the spectral width with temperature is not due to a decrease of the ZFS parameter, *D*. Thus, analysis of the results requires that dynamic effects should be taken into account in the triplet line shape analysis. Two main approaches concerning the dynamics of the chromophore in its excited triplet state are feasible: (i) rotational diffusion model of the excited triplet chromophores[37,38] and (ii) discrete solidlike jumps model, which assumes exchange between two principal magnetic axes about the third principal axis.[17,18] With the bulky chromophores studied here and the relatively high-viscosity LCs, we rule out the first mechanism of rotational diffusion, thus leaving the discrete solidlike jumps model as a possible mechanism. Therefore, line shape analysis was carried out by utilizing eqs 2 and 3, assuming the anisotropic distribution of the H_2*t*TETPP in the LC with $D > 0$ (Table 2). It is noteworthy that the reduction of the spectral width (for **L**||**B**) from 305 G (low temperature) to 215 G (high temperature) is by a factor of $1.4 = \sqrt{2}$. This is exactly the reduction in the line width of the $(Bchl)_2^{\bullet+}$ special pair in photosynthesis.[39] Moreover, the apparent reduction of *D* upon increasing the temperature by a factor of 1.4 implies an increase of almost 23% in the π-system dimensions. Such an increase is unlikely to result from conformational changes in H_2*t*TETPP, confirming our suggestion that intermolecular energy transfer is the mechanism to account for the spectral changes in E-7.

We describe now the spectral changes in terms of the discrete solidlike jumps model. Already at 140 K the analysis shows that the exchange between *X* and *Z* axes occurs about the *Y* canonical orientation with a rotational angle of 35°. Increasing the temperature to the soft crystalline phase ($T = 255$ K), rotational angle about *Y* increases to 50° (Table 2). In the nematic fluid phase (288 K) the removal of motional restrictions allows for additional degrees of freedom, which affect the dynamics. Thus, in addition to the exchange about *Y* canonical orientation, an exchange about the *Z* principal axes starts to be significant, with a rate of $1.4 \times 10^7\ s^{-1}$. At even higher temperatures (326 K) close to the isotropic phase, the exchange rate is higher by 1 order of magnitude, i.e., $k = 3.36 \times 10^8\ s^{-1}$, as compared to all low-temperature rates. Such a noticeable change of rates is reflected by the narrow width of the triplet spectrum (Figure 6). The line width variations are certainly due to increasing the probability of energy transfer, as the movement of the solvent and solute molecules increases.

The triplet spectra of the cis-isomer, H_2*c*TETPP, are shown in Figure 7. Although the line shape of this compound is different from that of the trans-isomer, it undergoes a similar exchange process. Also here, simulations of the triplet spectra were carried out by taking into account the triplet exchange expressed by the rotation angles about the different principal axis. Thus, in the temperature range of 140 K < *T* < 273 K,

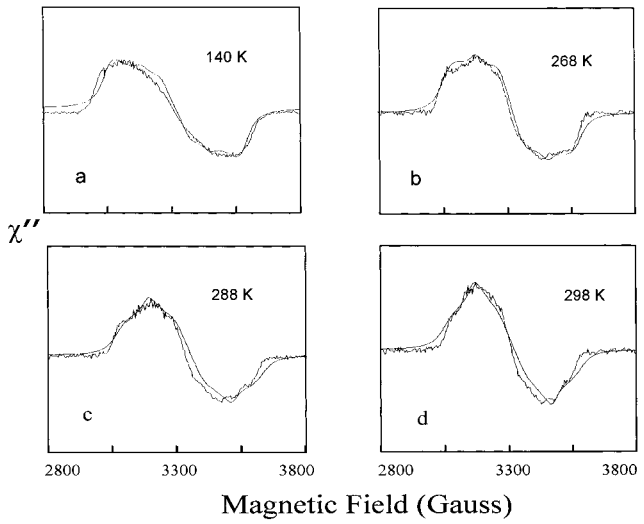

Figure 7. Temperature dependence of TREPR spectra (**L**||**B**), of H_2*c*ETPP in the crystalline and nematic phases of E-7, taken at 850 ns after the laser pulse. Other experimental conditions are as in Figure 3. The superimposed smooth curves are computer simulations according to eqs 2 and 3 with parameters given in Tables 1 and 2.

the triplet dynamics are best described by 90° jumps about *Z*, while the other rotations about *X* and *Y* contribute slightly to the dynamics. The exchange rates at different temperatures are presented in Table 2. When the temperature increases, the line shape of the detected spectra at the **L**||**B** orientation is changed, again due to an increase of the exchange rate from 1.4×10^7 to 7×10^7 s^{-1} at 140 and 298 K, respectively. The difference in the dynamic behavior between cis- and trans-isomers in E-7 may be attributed to the different symmetries of these chromophores. It should be noted that the observed 90° jumps about the *Z* principal axes in the case of H_2*c*TETPP reflects the cis configuration of the chromophore (Figure 1), where the in-plane axes *X* and *Y* are almost identical. On the other hand, the symmetry of the trans-isomer leads to less restricted rotational jumps, as indeed confirmed by the analysis.

(d) H_2OETPP in LC. The triplet spectra of H_2OETPP in E-7 at the **L**||**B** orientation as a function of temperature are shown in Figure 8. Similar to the compounds discussed earlier, the spectral changes are attributed to energy transfer between neighboring molecules. Inspection of Table 2 shows that the rate of the energy transfer at 140 K < *T* < 273 K is 5.6×10^6 s^{-1}, and the main exchange occurs about the short axis *Z* ($|D| = 3|E|$ and $D > 0$). At $T > 280$ K a dramatic change in the triplet line shape, different from the previously described compounds is noticed. An additional spectrum starts to emerge with the same spectral width as the low-temperature one (Figure 8). Further raising of the temperature results in a gradual disappearance of the inner broad spectrum, and at $T > 310$ K it completely vanishes, leaving only the outer lines. This spectrum is well simulated by the solidlike rotation about the *Y* principal axis, which is the long axis. This is analogous to the case treated previously for the triplet dynamics of C_{70}.[28] We attribute this change in rotation to increasing the degrees of freedom at the fluid nematic phase of E-7. In Figure 8c we show the triplet spectrum of H_2OETPP, detected at $T = 268$ K. This spectrum can be simulated by summing up the spectra detected at $T = 255$ K and that detected at 326 K in the ratio 1:1.1. The assignment of the two spectra to different species is consistent with the different kinetic traces taken at the field positions **A** and **B** (Figure 8). As to the origin of the two species, we attribute them to different triplet conformers of H_2OETPP, exhibiting different line shapes, while retaining as expected, the same ZFS parameters *D* and *E*. This observation is in line with equilibrium among various conformers,

$$S_I \leftrightarrow S_{II} \tag{11}$$

and is consistent with previous NMR and EPR studies.[4,10,12]

(e) Magnetophotoselection Experiments. The results presented in the previous sections show that the triplet manifold of the distorted porphyrins demonstrate noticeable differences as compared to H_2TPP. For instance, we have found that the polarization pattern of the triplet spectra and the sign of the ZFS parameter, *D*, depend on the number of ethyl substituents. In addition, one of the goals of this study is to understand how molecular distortions affect the mutual relationship between triplet spin alignment and the sign of ZFS parameter, *D*. It is known that $D < 0$ corresponds to head-to-tail spin alignment in the triplet state, while the side-by-side spin configuration corresponds to $D > 0$.[40] With this in mind we have performed MPS experiments, which enable us to determine the absolute sign of *D* by having known the location of **M** in the magnetic frame of reference. Normally, in planar aromatics the location of **M** is in the molecular plane, such that the *Z* canonical orientation of the ZFS tensor is perpendicular to it. Upon molecular distortions, the location of **M** in the magnetic frame of reference as well as the triplet spin alignment may change. Thus, when the angle between the **M** and *Z* canonical orientation (γ) is less than ~54.5°, then $D < 0$.[25] As will be shown below, MPS experiments indicate that $D > 0$ in all four distorted triplet porphyrins.

In the MPS experiments the degree of polarization, R_i, for each canonical orientation, *i*, is defined by[25]

$$R_i = [(I_{||} - I_{\perp})/(I_{||} + I_{\perp})]_i \tag{12}$$

where *I* is the EPR signal intensity for the vertical or parallel light polarizations. A positive value of R_i implies that the corresponding *i* axis is close to the **M**. In Figure 9 we show the triplet spectra of H_2DETPP, H_2*c*TETPP, H_2*t*TETPP, and H_2-OETPP dissolved in toluene, with two directions of the electric field vector, i.e., **E**||**B** and **E**⊥**B**. The triplet spectrum of H_2-DETPP (Figure 9a,b), in terms of the EPR intensity ratio, strongly depends on the light polarization. Applying eq 12 to the spectra results in a negative R_i for the *Z* canonical orientation. Therefore, the orientations *X* and *Y* are close to **M**. Since the location of **M** is unknown, we have carried out a line shape analysis of the triplet spectra by employing eqs 1 and 4−6. The angle γ between the **M** and *Z* canonical orientation, extracted from the line shape analysis is $\gamma = 80 \pm 5°$ (Table 3), i.e., $D > 0$. It is noteworthy that within the point dipole approximation D [$\propto(1-3\cos^2\gamma)/r^3$] is positive for $\gamma > 54.5°$.

In the case of H_2*c*TETPP and H_2*t*TETPP (Figure 9c−f) the triplet spectra taken with **E**||**B** and **E**⊥**B** polarization of the laser are similar. Therefore, the utilization of eq 12 is meaningless. In other words, the location of **M** is such that the spectra at **E**||**B** and **E**⊥**B** are very similar. Such a result is obtained for particular γ and δ angles (Figure 2), as verified by the line shape analysis. Indeed, a good agreement between the theory and the experiment was observed and the angle, γ, between **M** and *Z*, is calculated to be $\gamma = 65 \pm 7°$ and $70 \pm 7°$ for H_2*c*TETPP and H_2*t*TETPP, respectively. These results, where **M** deviates slightly from the *X*, *Y* plane, are in line with the more distorted cis and trans porphyrins as compared to H_2DETPP. Finally, in the case of H_2OETPP, the deviation is even more noticeable. The calculated angle γ between **M** and the *Z* canonical

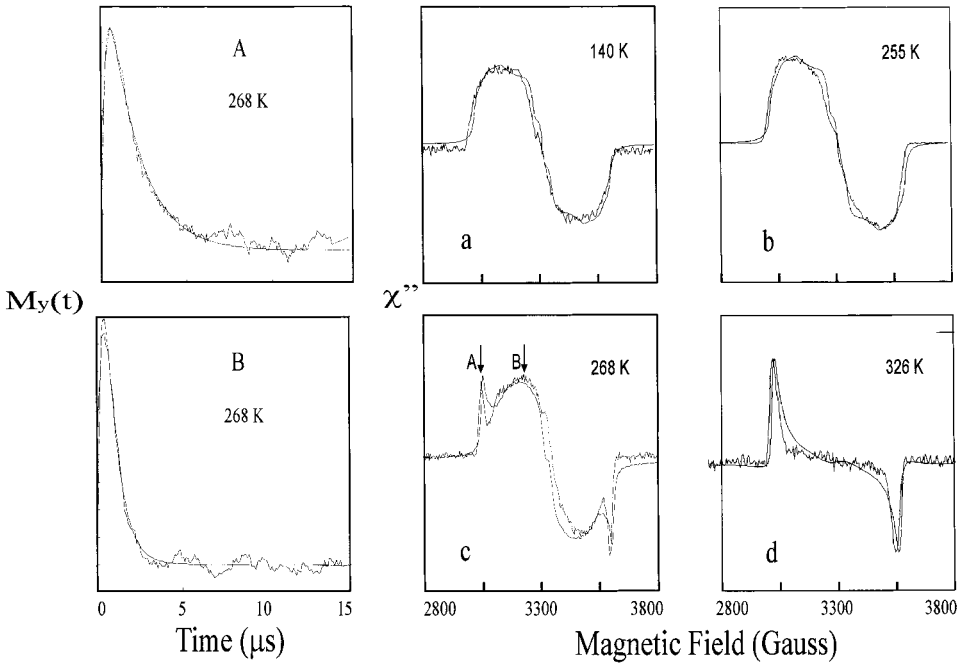

Figure 8. Right: Temperature dependence of TREPR spectra of H_2OETPP in the crystalline and nematic phases of E-7 (**L**||**B**), taken at 850 ns after the laser pulse. Other experimental conditions are as in Figure 3. The superimposed smooth curves (a), (b), and (d) are computer simulations according to eqs 2 and 3. Summation of spectra b and d in the ratio 1:1.1 are shown in (c). Left: Kinetic profiles of the magnetization $M_y(t)$, taken at the **A** (top) and **B** (bottom) field positions of the triplet spectrum (c), at a microwave power of 50 mW. The solid lines superimposed on the experimental curves are computer simulations according to eqs 8 and 9.

orientation, extracted from the line shape analysis is $\gamma = 55 \pm 5°$. Applying eq 12 to the spectra of Figure 9g,h results in a positive R_i for the inner line. Therefore, the canonical axis X associated with this line is close to **M**. To conclude, in all compounds the calculated angles obey the relation, $\gamma \geq 55°$ implying that $D > 0$ and the spin alignment, to a good approximation, is side-by-side.

It should be noted that the electronic absorption spectra of the investigated porphyrins are red-shifted as the macrocycle distortions increase. As was reported recently,[8] this is due to destabilization of the $\pi-$system, which mainly results in an increase of the HOMO level. The following order of nonplanarity was obtained: H_2OETPP > H_2cTETPP > H_2tTETPP > H_2DETPP with average deviations of the 24 macrocycle atoms from their least-squares plane of 0.54, 0.38, 0.29, and 0.1 D, respectively.[41] It is in line with our observation that the angle between the X, Y magnetic plane and **M** is $(90° - \gamma)$, which increases with the number of ethyl substituents (Table 3).

VI. Conclusion

The porphyrins examined in this work are characterized by different degrees of molecular distortions, resulting in different polarization patterns, thus affecting the spin density distribution. In the LC matrixes anisotropic distribution and packing lead to intermolecular energy transfer between the neighboring molecules. We have demonstrated that the LC matrix allows these dynamic effects to be probed over a wide range of temperatures. In the case of H_2DETPP it was shown that the population and decay rates among the three triplet sublevels are anisotropic. This observation manifests itself through the geometrical distortion. The largest deviation from planarity is found in H_2-OETPP, which leads to the simultaneous presence of two different conformers. In addition to above results, we have determined by MPS technique the location of the optical transition moment, which is related to the molecular distortions, spin alignment and sign of the ZFS parameter, D. Thus, analysis

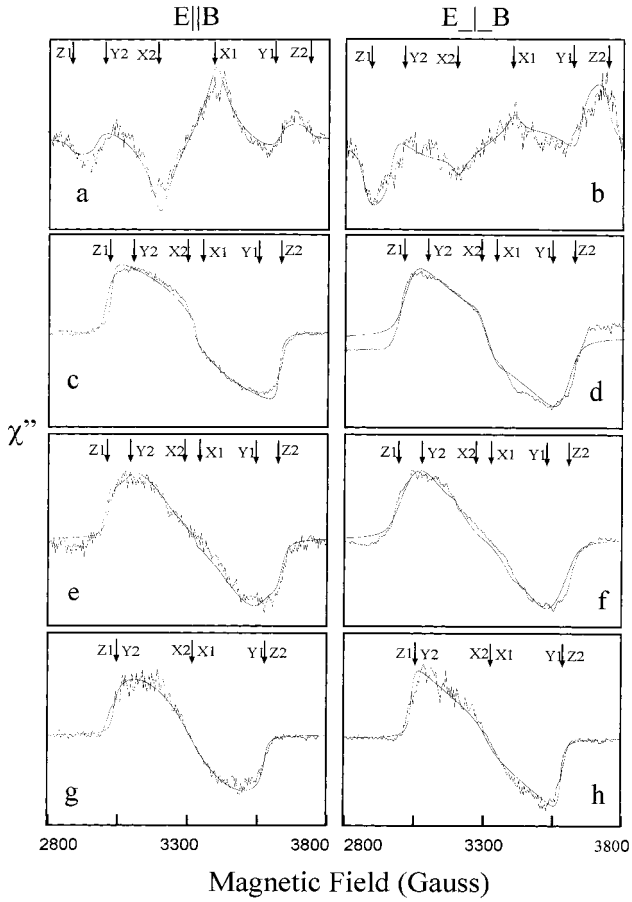

Figure 9. MPS time-resolved triplet EPR spectra of H_2DETPP (a), (b); H_2cTETPP (c), (d); H_2tTETPP (e), (f), and H_2OETPP (g), (h), randomly oriented in toluene glass. Pulsed laser excitation (**E**||**B**) and (**E**⊥**B**) at 532 nm, 12 mJ/pulse. The smoothed curves are simulations obtained by employing eqs 1, 4, and 5 and the parameters extracted from the line shape analysis are presented in Table 3.

TABLE 3: Parameters of Triplet States and Location of the Optical Transition Moment of Distorted Porphyrins in Toluene

compound	D^a	E^a	A_X:A_Y:A_Z	γ^b	δ^b
H_2DETPP	428	80	1:0.1:0	80	25
H_2cTETPP	310	70	0.2:0.1:1	65	70
H_2tTETPP	315	72	0.7:0.3:1	70	70
H_2OETPP	277	92	0.2:0.5:1	55	20

[a] $\times 10^4$ (cm^{-1}) (error $\pm$ 5). [b] In degrees (error $\pm$ 5°).

of the results enables us to determine that (i) the location of **M** is out of the *X*, *Y* plane of the ZFS tensor and (ii) the sign of the ZFS parameter, *D*, is positive and with side-by-side spin alignment as in typical $\pi\pi^*$ transitions.

Finally, this study exemplifies how molecular distortions and conformational variation affect photophysical and photochemical properties of substituted porphyrins. As shown in photosynthetic reaction centers, relatively small distortions of the molecular systems in the protein environment can lead to large changes in spin densities. This point has been verified by TREPR with the model porphyrinoid systems studied here.

Acknowledgment. This work was supported by the U.S.-Israel BSF, the Deutche Forschungsgemeinschaft (Sfb 337), and a grant of the Ministry of Science in Israel and the Forschungszentrum Jülich GmbH (KFA) in Germany. The Farkas Center is supported by the Bundesministerium für Bildung und Forschung and the Minerva Gesellschaft für Forschung GmbH, Germany. This work is in partial fulfillment of the requirements for a M. Sc. degree (S.S.) at the Hebrew University of Jerusalem. M.O.S. gratefully acknowledged generous financial support from the Deutsche Forschungsgemeinschaft (Se543/2-4 and Heisenberg scholarship Se543/3-1) and the Fonds der Chemischen Industrie.

References and Notes

(1) Deisenhofer, J.; Epp, O.; Miki, K.; R. Huber; Michel, H. *Nature* **1985**, *318*, 618.

(2) Tronrud, D. E.; Schmid, M. F.; Matthews, B. W. *J. Mol. Biol.* **1986**, *188*, 443.

(3) Barkigia, K. M.; Renner, M. W.; Furenlid, L. R.; Medforth, C. J.; Smith, K. M.; Fajer, J. *J. Am. Chem. Soc.* **1993**, *115*, 3627.

(4) Medforth, C. J.; Senge, M. O.; Smith, K. M.; Sparks, L. D.; Shelnutt, J. A. *J. Am. Chem.* Soc. **1992**, *114*, 9859.

(5) Kratky, C.; Dunitz, J. *J. Mol. Biol.* **1977**, *113*, 431.

(6) Scheidt, W. R.; Lee, Y. J. In *Structure and Bonding*; Buchler, J. W., Ed.; Springer-Verlag: Berlin, 1987; Vol. 64, p 1.

(7) Barkigia, K. M.; Fajer, J. In *The Photosynthetic Reaction Center*; Deisenhofer, J., Norris, J. R., Eds.; Academic Press: San Diego, 1993; Vol. II, p 513.

(8) Barkigia, K. M.; Chantranupong, L.; Smith, K. M.; Fajer, J. *J. Am. Chem. Soc.* **1988**, *110*, 7566.

(9) Gudowska-Nowak, E.; Newton, M. D.; Fajer, J. *J. Phys. Chem. A* **1990**, *94*, 5795.

(10) Barkigia, K. M.; Berber, M. D.; Fajer, J.; Medforth, C. J.; Renner, M. W.; Smith, K. M. *J. Am. Chem. Soc.* **1990**, *112*, 8851.

(11) Mandon, D.; Ochsenbein, P.; Fischer, J.; Weiss, R.; Jayaraj, K.; Austin, R. N.; Gold, A.; White, P. S.; Brigaud, O.; Battioni, P.; Mansuy, D. *Inorg. Chem.* **1992**, *31*, 2044.

(12) Shelnutt, J. A.; Medforth, C. J.; Berber, M. D.; Barkigia, K. M.; Smith, K. M. *J. Am. Chem.* Soc. **1991**, *113*, 4077.

(13) Biczok, L.; Linschitz, H. Private communication.

(14) Gentemann, S.; Nelson, N. Y.; Jaquinod, L.; Nurco, D.; Leung, S. H.; Medforth, C. J.; Smith, K. M.; Fajer, J.; Holten, D. *J. Phys. Chem. A* **1997**, *101*, 1247.

(15) Regev, A.; Galili, T.; Medforth, C. J.; Smith, K. M.; Barkigia, K. M.; Fajer, J.; Levanon, H. *J. Phys. Chem. A* **1994**, *98*, 2520.

(16) Regev, A.; Levanon, H.; Murai, T.; Sessler, J. L. *J. Chem. Phys.* **1990**, *92*, 4718.

(17) Regev, A.; Galili, T.; Levanon, H. *J. Chem. Phys.* **1991**, *95*, 7907.

(18) Regev, A.; Gamliel, D.; Meiklyar, V.; Michaeli, S.; Levanon, H. *J. Phys. Chem. A* **1993**, *97*, 3671.

(19) Kalisch, W. W.; Senge, M. O. *Tetrahedron Lett.* **1996**, *37*, 1183.

(20) E-7 is a eutectic mixture of R_i−C_6H_5−C_6H_5−CN: $R_1 = C_5H_{11}$ (51%); $R_2 = C_7H_{15}$ (25%); $R_3 = C_8H_{17}O$ (16%); $R_4 = C_5H_{11}C_6H_5$ (8%).

(21) Gonen, O.; Levanon, H. *J. Phys. Chem. A* **1985**, *89*, 1637.

(22) Regev, A.; Berman, A.; Levanon, H.; Murai, T.; Sessler, J. L. *Chem. Phys. Lett.* **1989**, *160*, 401.

(23) El-Sayed, M. A.; Siegel, S. *J. Chem. Phys.* **1966**, *44*, 1416.

(24) Thurnauer, M. C.; Norris, J. R. *Biochem. Biophys. Res. Commun.* **1976**, *73*, 501.

(25) Regev, A.; Michaeli, S.; Levanon, H.; Cyr, M.; Sessler, J. L. *J. Phys. Chem. A* **1991**, *95*, 9121.

(26) Shain, A. L. *J. Chem. Phys.* **1972**, *56*, 6201.

(27) Gonen, O.; H. Levanon, H. *J. Chem. Phys.* **1986**, *84*, 4132.

(28) Levanon, H.; Meiklyar, V.; Michaeli, S.; Gamliel, D. *J. Am. Chem. Soc.* **1993**, *115*, 8722.

(29) Hore, P. J.; McLauchlan, K. A. *J. Magn. Reson.* **1979**, *36*, 129.

(30) Hore, P. J.; McLauchlan, K. A. *Rev. Chem. Intermed.* **1979**, *3*, 89.

(31) Berman, A.; Michaeli, A.; Feitelson, J.; Bowman, M. K.; Norris, J. R.; Levanon, H.; Vogel, E.; Koch, P. *J. Phys. Chem. A* **1992**, *96*, 3041.

(32) Michaeli, S.; Hugerat, M.; Levanon, H.; Bernitz, M.; Natt, A.; Neumann, R. *J. Am. Chem.* Soc. **1992**, *114*, 3612.

(33) It is important to point out that in a previous paper (ref 15) the polarization pattern of triplet H_2OETPP was found to be **e,e,e,a,a,a**. This pattern is opposite to that found in the present work. Moreover, the ground-state absorption spectrum of H_2OETPP in both experiments was found to be identical. Facing this apparent discrepancy, we have checked carefully the polarization features by running the experiments with fresh samples from different sources. As described in the text the polarization pattern of **a,a,a,e,e,e** is consistent with the results of the distorted porphyrins. It is evident that the polarization pattern is very sensitive to the value of γ about 55°. Thus, a very slight increasing of the molecular distortion (e.g., sample preparation) may lead a phase inversion via a change in γ, i.e., $\gamma < 55°$.

(34) Hasharoni, K.; Levanon, H.; von Gersdorff, J.; Kurreck, H.; Möbius, K. *J. Chem. Phys.* **1993**, *98*, 2916.

(35) Terazima, N.; Hirota, H.; Shimohara, Y.; Saito, Y. *Chem. Phys. Lett.* **1992**, *195*, 333.

(36) The temperature dependence of the perpendicular spectra is not shown, since a realignment process of the LC director, from the perpendicular to the parallel orientation, occurs at temperatures above 240 K.

(37) Gamliel, D.; Levanon, H. *J. Chem. Phys.* **1992**, *97*, 7140.

(38) Gamliel, D.; Levanon, H. *Stochastic Processes in Magnetic Resonance*; World Scientific: Singapore, 1995.

(39) Feher, G. *Photosynth. Res.* **1998**, *55*, 3.

(40) Levanon, H.; Norris, J. R. *Chem. Rev.* **1978**, *78*, 185.

(41) Senge, M. O.; Kalisch, W. W. *Inorg. Chem.* **1997**, *36*, 6103.